Supporting Information

Core-Shell Switching 3D Printing for Soft Electronics

Jeonghoon Lee, Riley Park, Denyse Isingizwe, Renkun Wang, Min Ku Kim, and Alex Chortos**

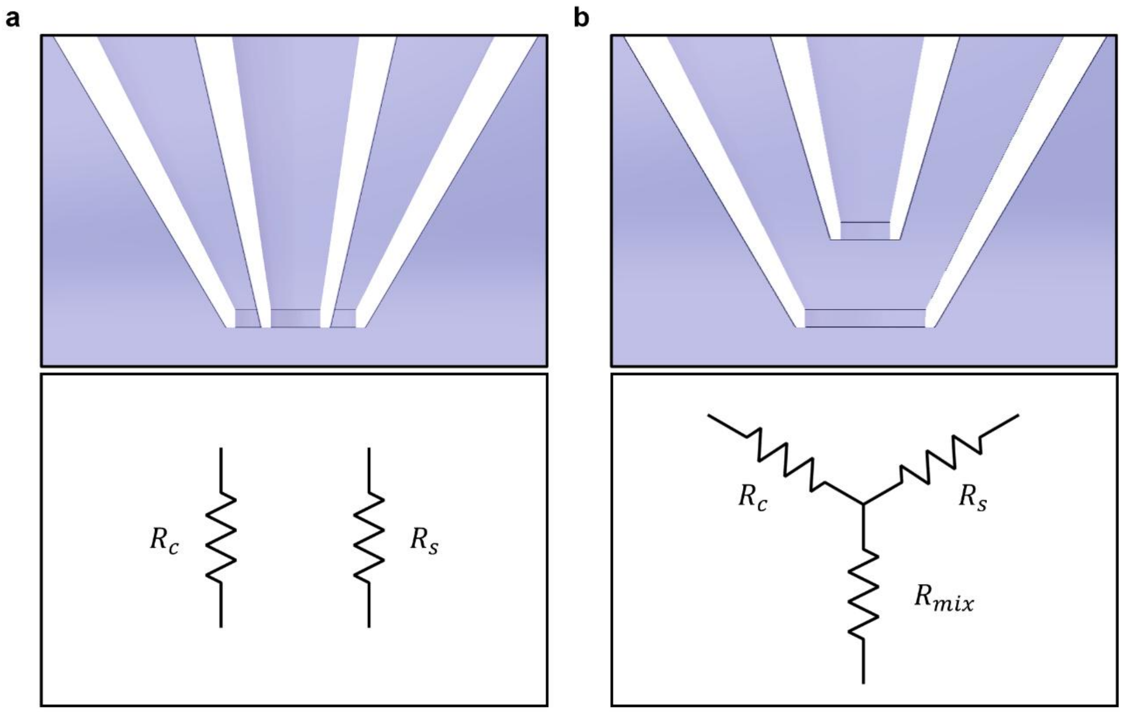

Figure S1. Simplified equivalent resistive network models of core shell flow. (a) Flat nozzle and (b) retracted nozzle.

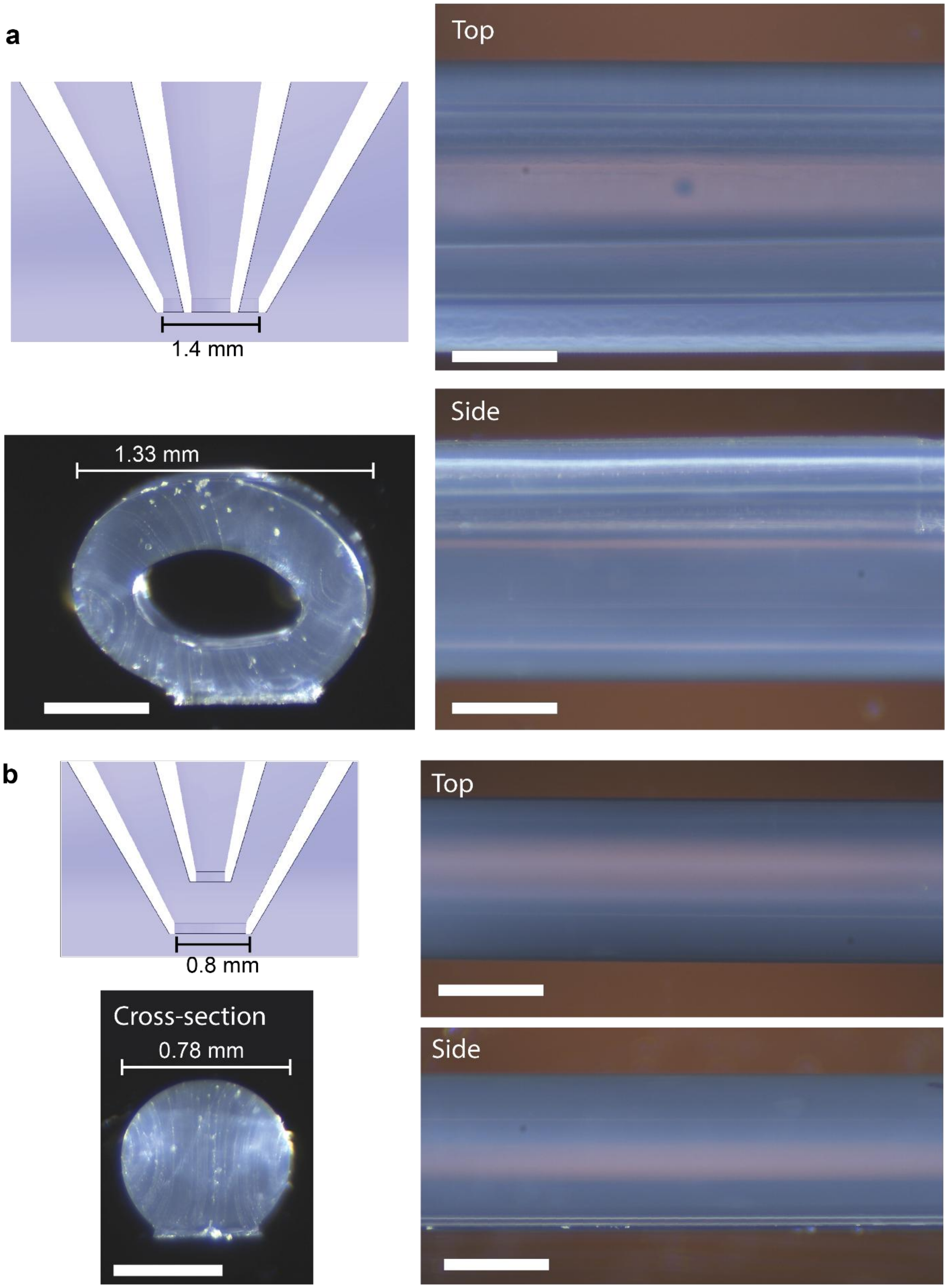

Figure S2. Geometrical characterization of shell-only filaments. (a) Flat nozzles produce hollow filaments while (b) retracted nozzles produce solid filaments. All scale bars are 0.5 mm.

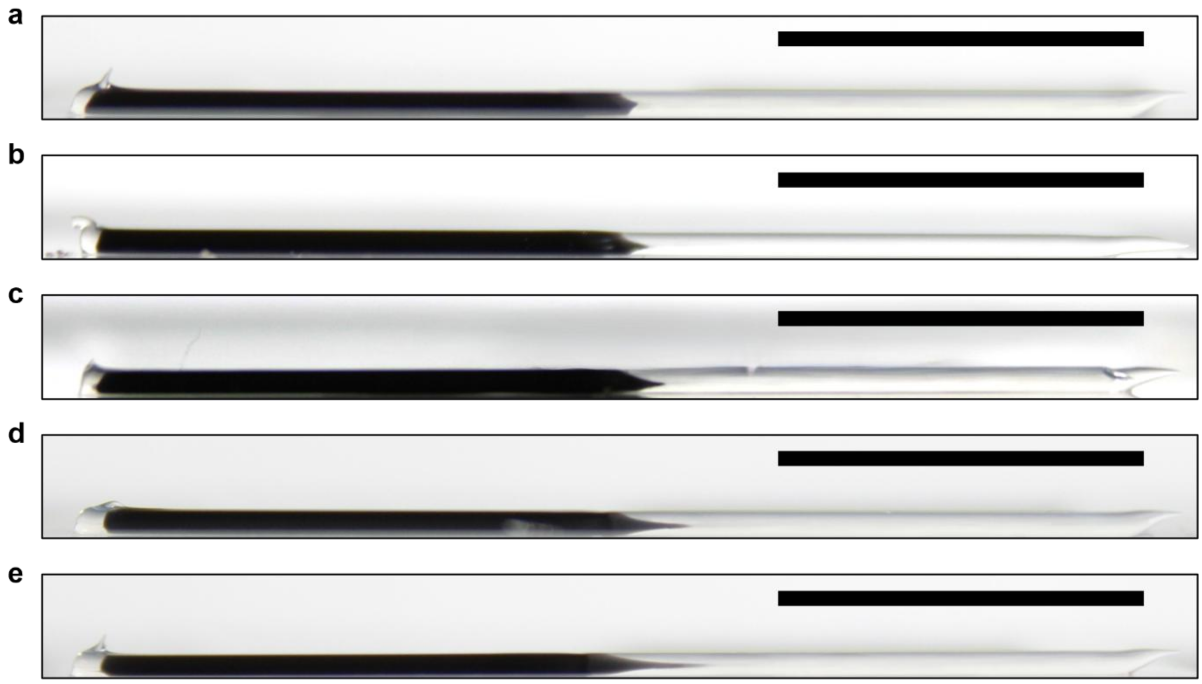

Figure S3. Raw images of the printed fibers (Core-only mode to shell-only mode) with different nozzle geometries (h values are varied) (a) h = 0.6 mm, (b) h = 0.8 mm, (c) h = 1.0 mm, (d) h = 1.2 mm, (e) h = 1.4 mm (Scale bar – 10 mm)

Supplementary Note 1: Linear model for flow through nozzles

The resistor model (Figure S1) includes two pressure inputs (P_c and P_s) and one node at which the pressure is floating (P_N). A model assuming linear relationships between the pressure and flow is given by:

$$\dot{m}_c + \dot{m}_s + \dot{m}_{mix} = 0$$

$$\frac{(P_c - P_N)}{R_c} + \frac{(P_s - P_N)}{R_s} + \frac{(0 - P_N)}{R_{mix}} = 0$$

$$\frac{P_c}{R_c} + \frac{P_s}{R_s} = P_N\left(\frac{1}{R_c} + \frac{1}{R_s} + \frac{1}{R_{mix}}\right)$$

We can measure the flow rate $\dot{m}_{mix}$ directly, giving a relation:

$$\dot{m}_{mix} = \frac{(P_c - P_N)}{R_c} + \frac{(P_s - P_N)}{R_s} = \frac{P_c}{R_c} + \frac{P_s}{R_s} + P_N\left(\frac{1}{R_c} + \frac{1}{R_s}\right)$$

To estimate the values of R_c and R_s, we make some additional assumptions. Since the length of the R_{mix} region is small, we expect that $R_{mix} << R_c,R_s$. If we set P_s to zero and assume negligible flow through R_s in that condition, then the relationship between P_c and $\dot{m}_{mix}$ can be used to estimate R_c.

$$[\dot{m}_{mix}]_{P_s=0} \approx \frac{P_c}{R_c} - \frac{P_N}{R_c} \approx \frac{P_c}{R_c} - \mathrm{K}$$

where K is assumed to be a constant. We leave this constant as an empirical value that includes the effect of the yield stress of the ink as well as the contribution of P_N/R_c.
This equation was used to fit the fluid flow rates for a nozzle with $w_1 = 0.6$, $w_2 = 0.8$, and $h = 1.0$ (Fig S4a and S4b), resulting in a linear model of:

$$\dot{m}_{mix} = \frac{P_c}{2.114} + \frac{P_s}{0.540} - 40.25$$

with P measured in psi and $\dot{m}$ measured in mg/s.
Next, the flow rate for different combinations of P_c and P_s were measured experimentally (Fig S4c and Fig S4d). The error between the measured and calculated flow rates are quantified by:

$$\%\, error = \frac{\dot{m}_{measured} - \dot{m}_{calculated}}{\dot{m}_{measured}} * 100$$

and the results are shown in Fig S4e. The simple linear model shows surprisingly good agreement (errors < 20%) with the measured flow rates considering that there are three large assumptions: (1) linear relationship between mass flow rate and pressure, (2) $R_{mix} << R_c,R_s$, and (3) no flow through $R_c(R_s)$ when P_c (P_s) is zero. In particular, the relationship between pressure and flow rate is typically highly non-linear, but can be close to linear when the wall shear stress (τ_w) is larger than the shear yield stress (τ_y) of the ink and the flow index of the ink is close to 1.[1]

The observation that the flow rate can be approximated as a linear combination of the flow through Rc and Rs suggest that the flow of each material through the interaction volume is operating in the flow control regime.

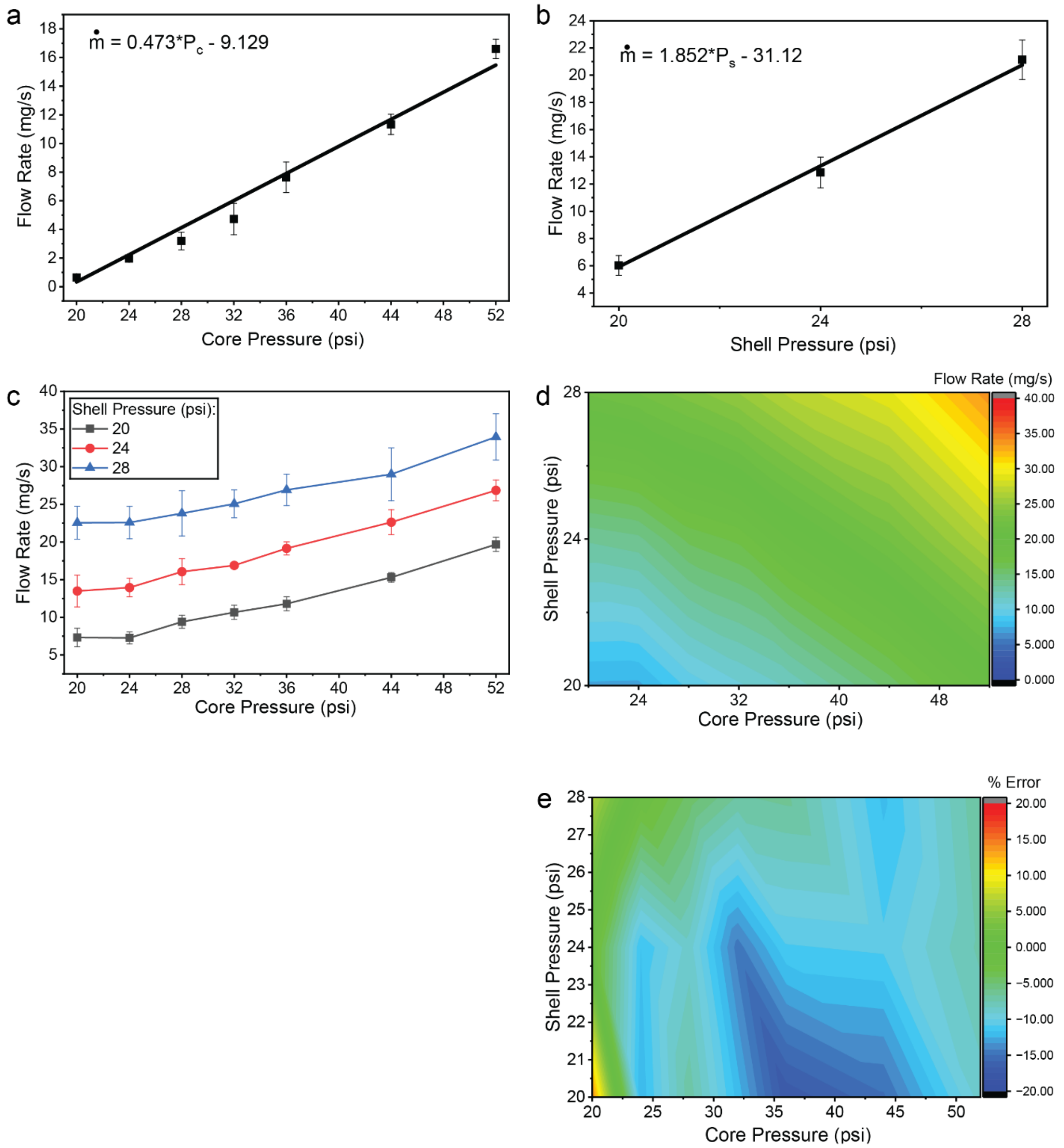

Figure S4. Experimental fitting of simplified equivalent resistive network model. (a) Flow rate through the core with the shell pressure set to zero. (b) Flow rate through the shell with the core pressure set to zero. Flow rate as a function of both core and shell pressures plotted as (c) a 2D graph and (d) a contour plot. (e) Contour map of the percent error between a simple linear resistive model and experimentally measured flow rates.

Supplementary Note 2: Calculation of interaction volume in the retracted core-shell nozzle

The interaction volume for a nozzle (Fig S5a) is calculated using the general equation for the volume of a cone ($V = \pi r^2 h/3$). For a nozzle with $w_1 = 0.6\ mm$ and $w_2 = 0.8\ mm$, the total height of the cone h_c is related to the retraction distance h by:

$$h_c = h + \frac{0.3}{\tan(30°)} = h + 0.52\ mm$$

The base radius of the cone is:

$$r = h_c \tan(30°)$$

The interaction volume is then:

$$V = \pi r^2 \left(\frac{h_c}{3}\right) - \pi (0.3)^2 \left(\frac{0.52}{3}\right)$$

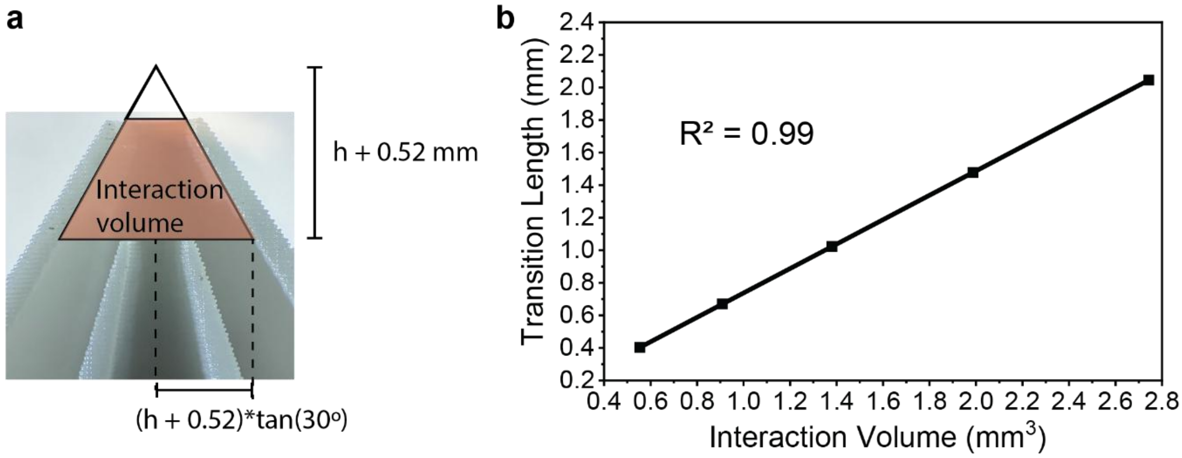

Figure S5. Correlating interaction volume with transition length. (a) Schematic of the calculation of the interaction volume. (b) Plot correlating the transition length with the interaction volume for the nozzle with $w_1 = 0.6\ mm$, $w_2 = 0.8\ mm$, and variable h (data shown in Figure 2e). The line represents a linear fit.

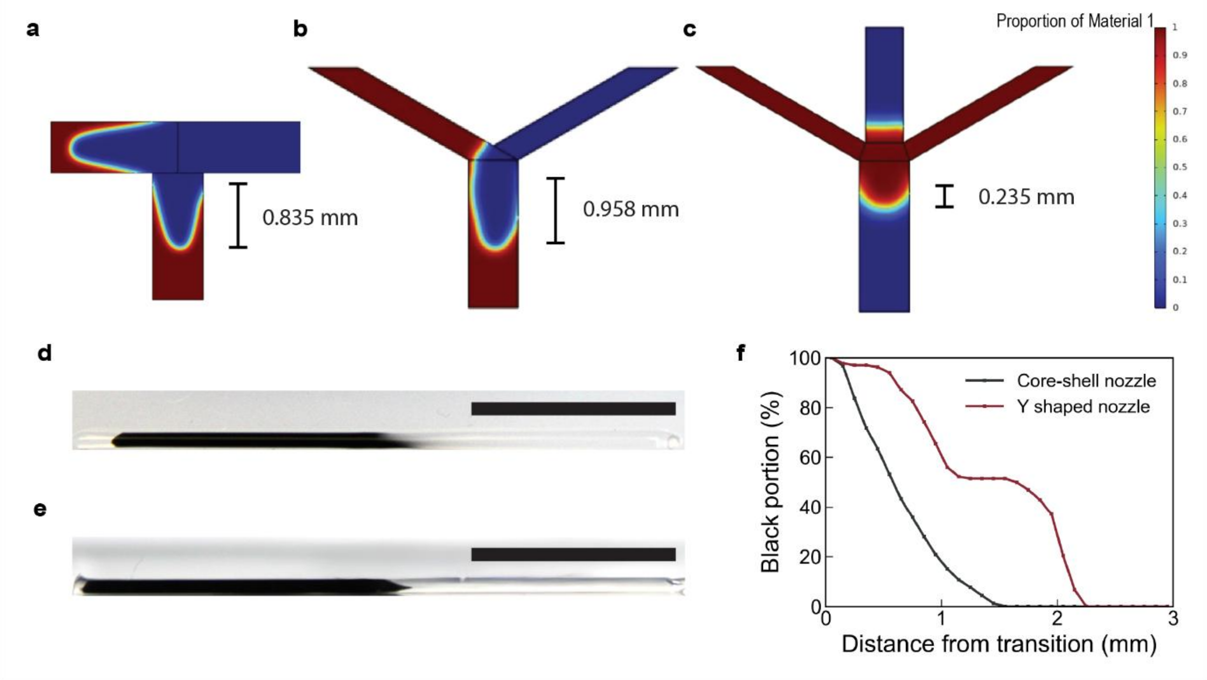

Figure S6. COMSOL simulations and experimental validation of material switching in nozzles with different geometries. (a) T-shaped switching junction, (b) Y-shaped switching junction, and (c) 2D nozzle geometry representing a core–shell nozzle, where the incoming material replaces the existing material from all sides during switching. (d) Experimental image of material switching printed using the Y-shaped nozzle. (e) Experimental image of material switching printed using the core–shell nozzle. (f) Quantitative analysis of the switching transition profile for the Y-shaped and core–shell nozzles. (Scale bar – 10 mm)

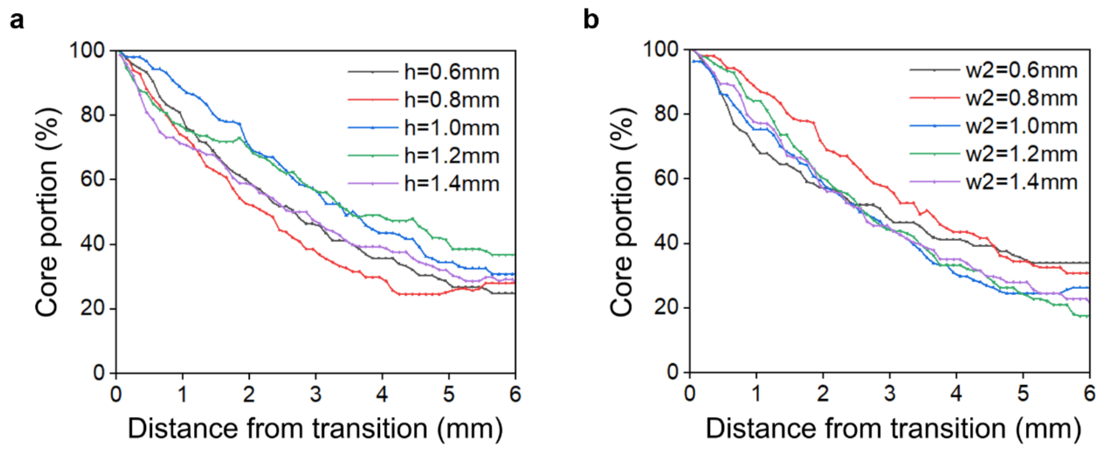

Figure S7. Transition of core-only print mode to core-shell print mode with different nozzle geometries (a) h variation with constant $w_2 = 0.8\ mm$, (b) w_2 variation with constant $h = 1.0\ mm$.

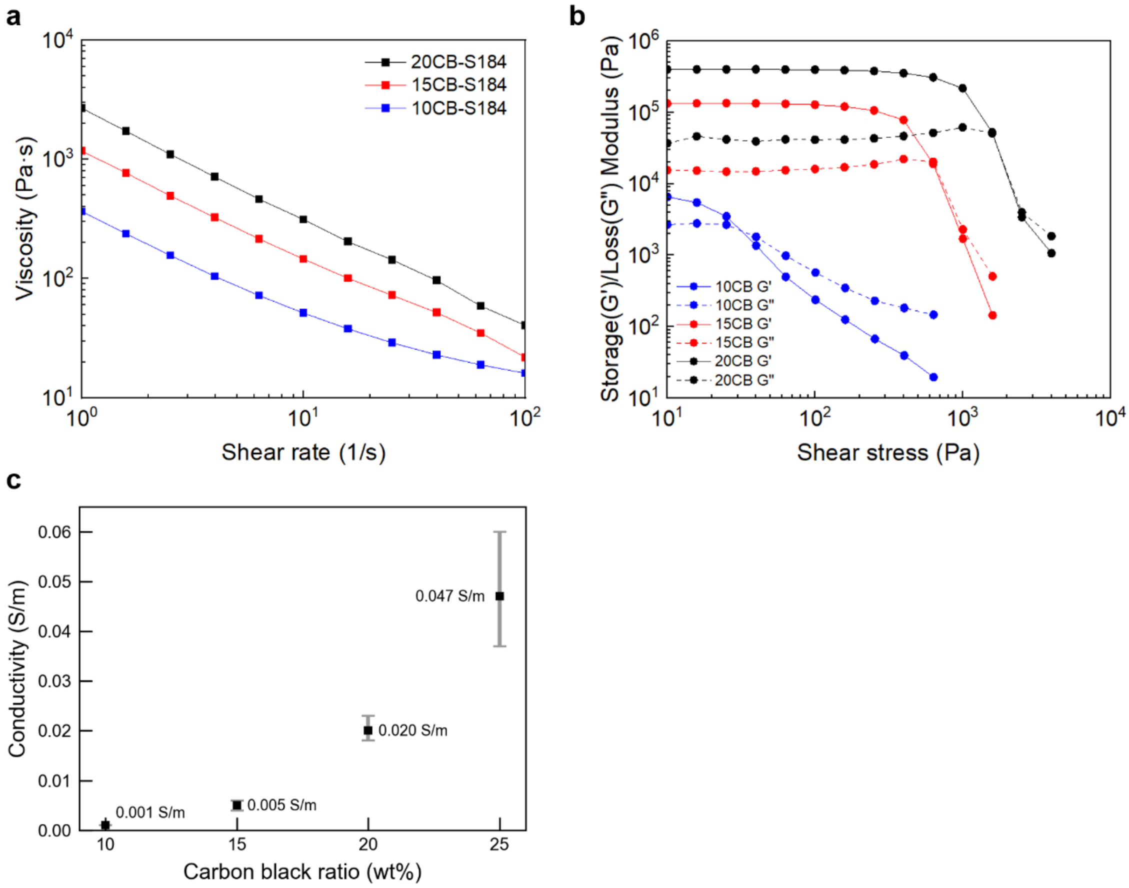

Figure S8. Rheological and electrical properties of conductive inks. (a) Viscosity vs shear rate, (b) Storage/loss modulus vs shear stress, (c) conductivity of conductive inks with different carbon black ratios.

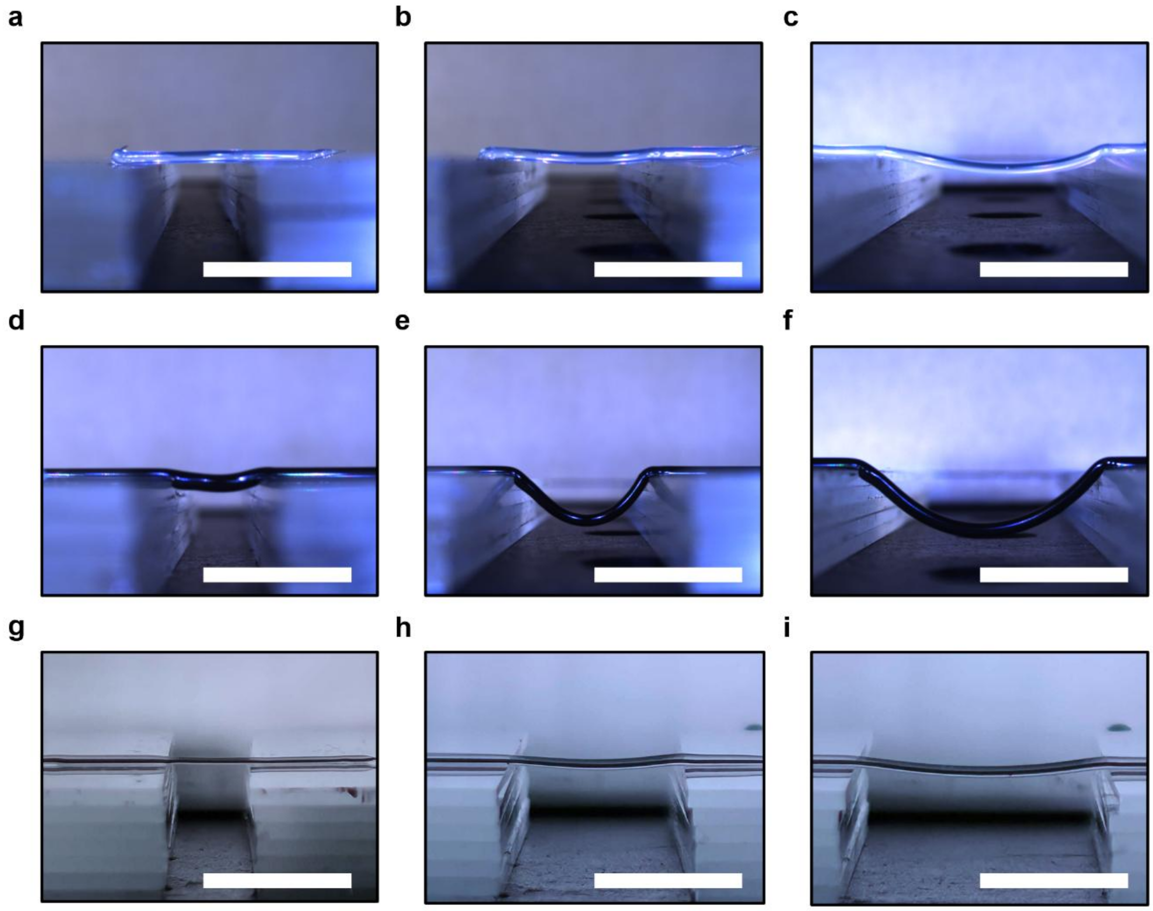

Figure S9. Bridging test of different print modes. Bridging behavior of shell-only mode (SE1700) across gap distances of (a) 5 mm, (b) 10 mm, and (c) 15 mm. Bridging behavior of core-only mode (Sylgard 184 incorporated with 20 wt% carbon black) across gap distances of (d) 5 mm, (e) 10 mm, and (f) 15 mm. Bridging behavior of core-shell mode across gap distances of (g) 5 mm, (h) 10 mm, and (i) 15 mm. (Scale bar – 10 mm)

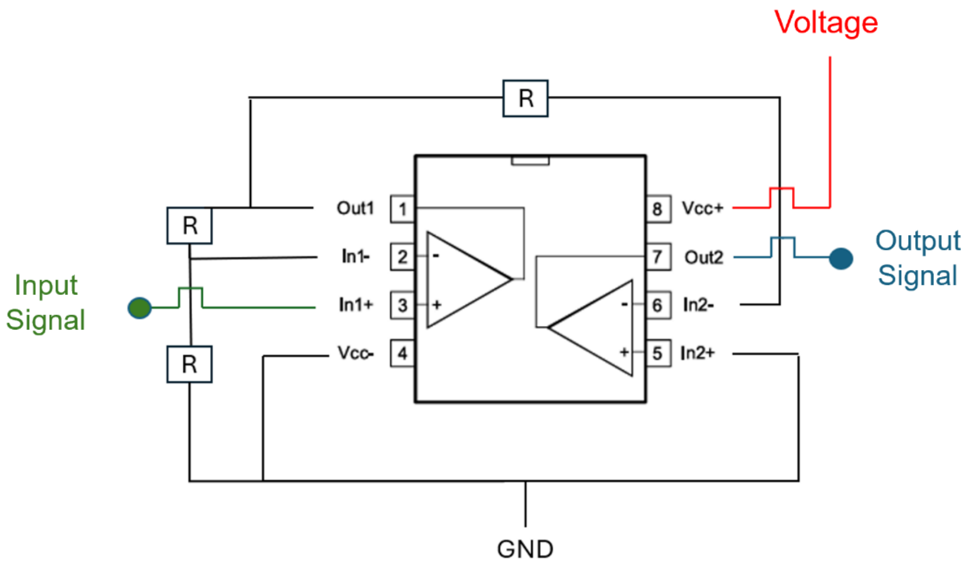

Figure S10. Circuit diagram of the two-stage operational amplifier.

References

[1] R. A. Chilton, R. Stainsby, *Journal of Hydraulic Engineering*. **1998**, 124, 5

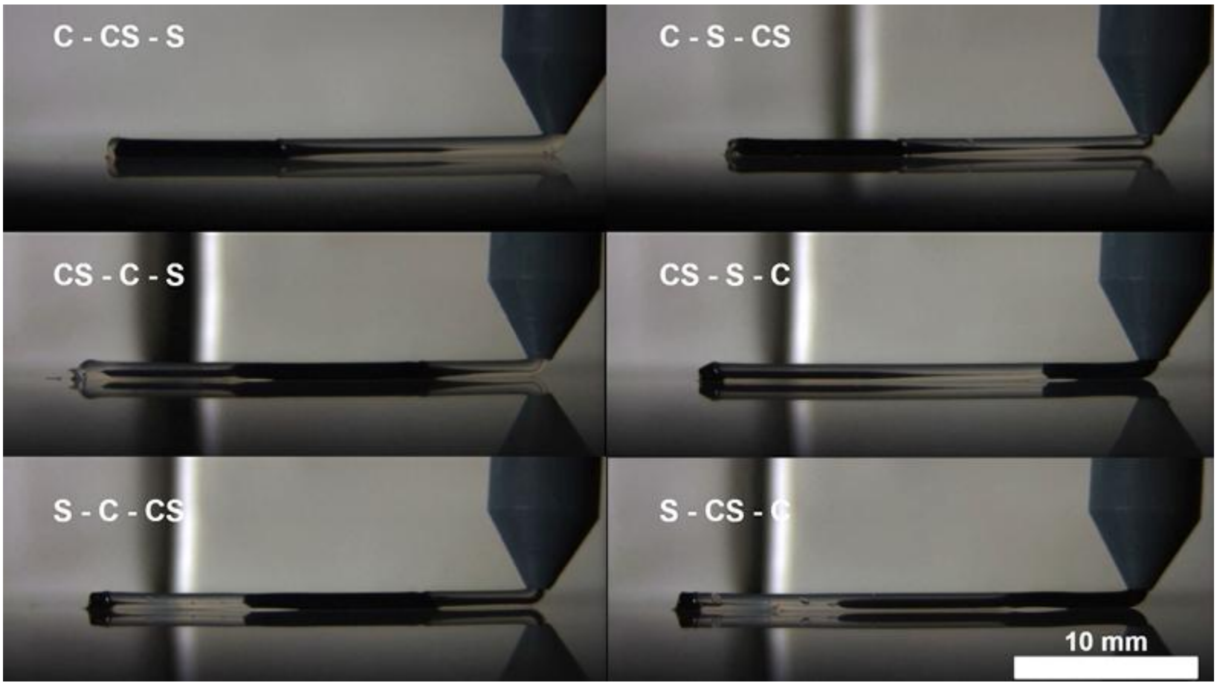

Supplemental Video 1. Core-shell switching 3D printing in 3 print modes (Scale bar: 10 mm)

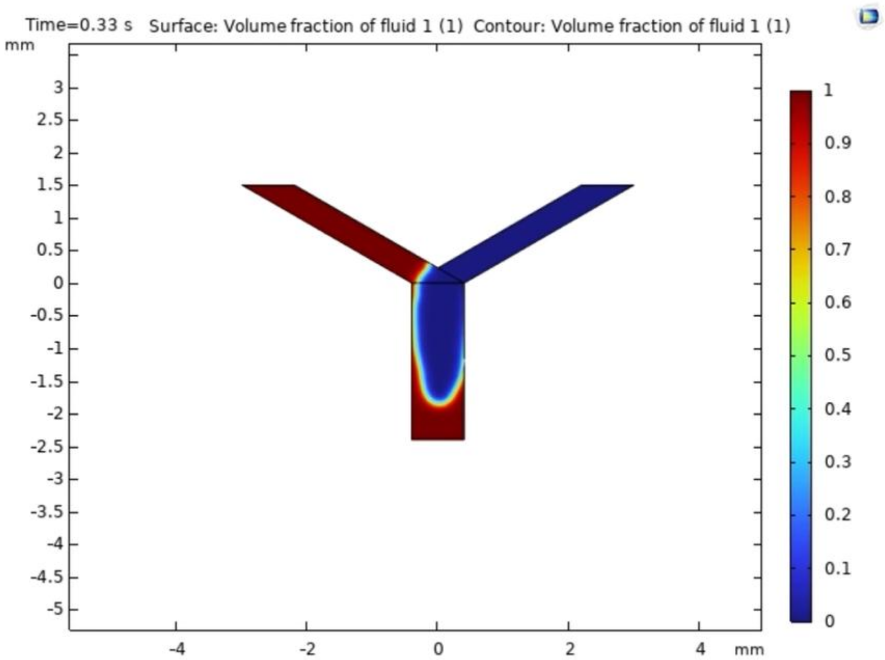

Supplemental Video 2. COMSOL simulations of the flow through switching nozzles with different geometries.

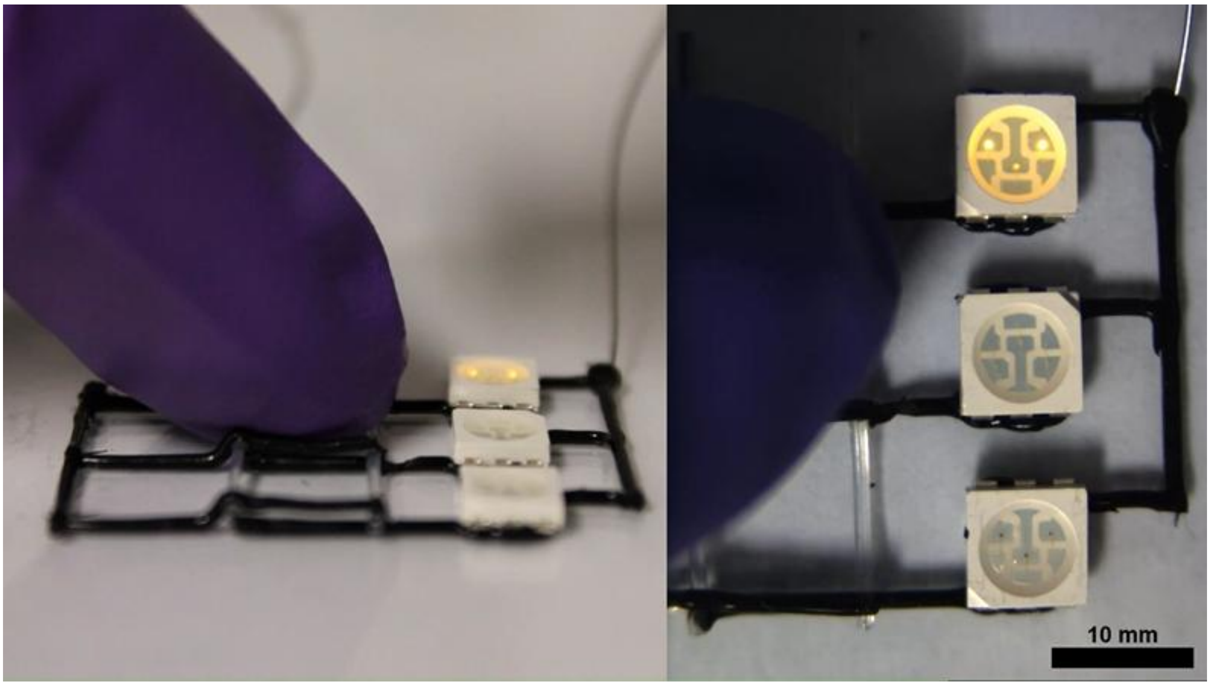

Supplemental Video 3. Soft analog switches made with core-shell switching 3D printing (Scale bar: 10 mm)

Supplemental Video 4. OR Gate made with core-shell switching 3D printing (Scale bar: 10 mm)

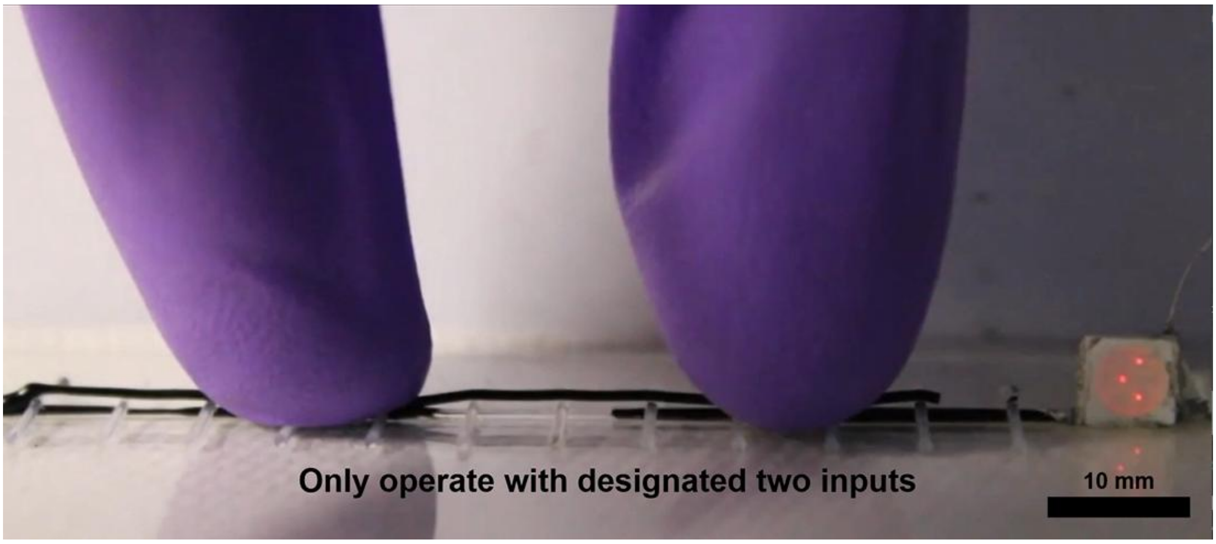

Supplemental Video 5. AND Gate made with core-shell switching 3D printing (Scale bar: 10 mm)

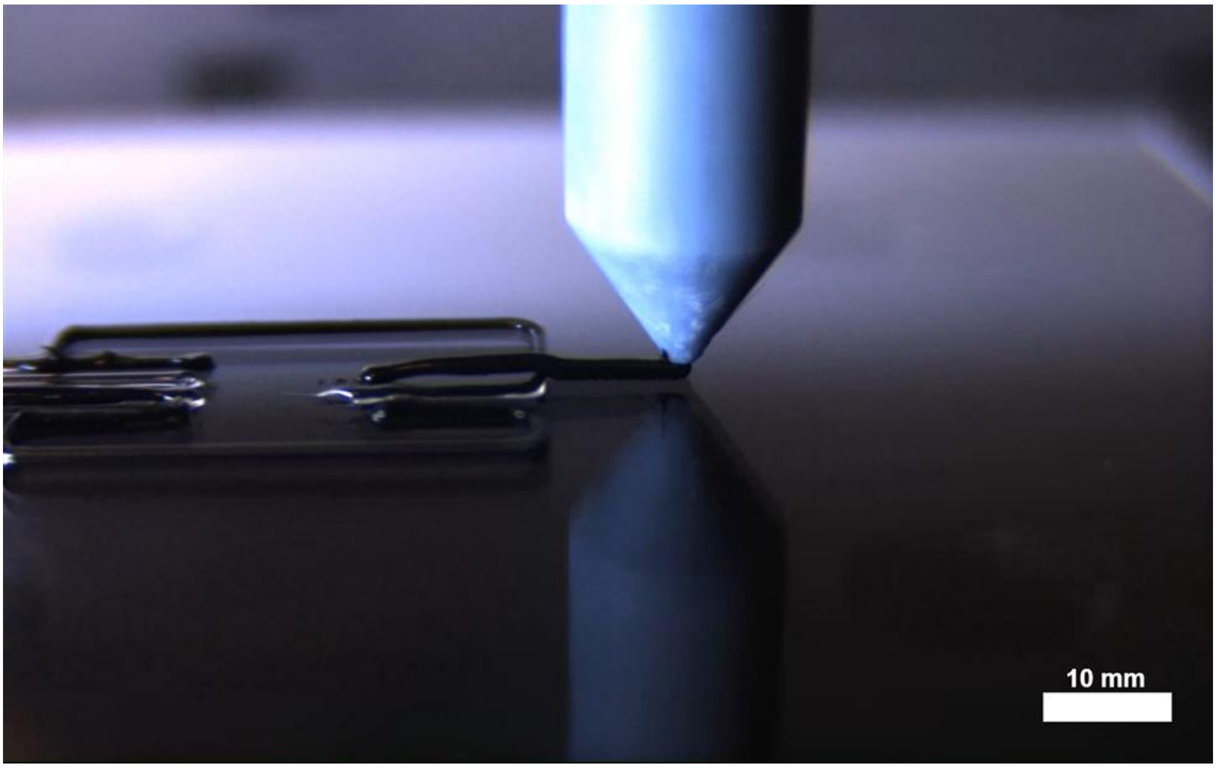

Supplemental Video 6. Printing the intersecting circuit for two-stage operational amplifier